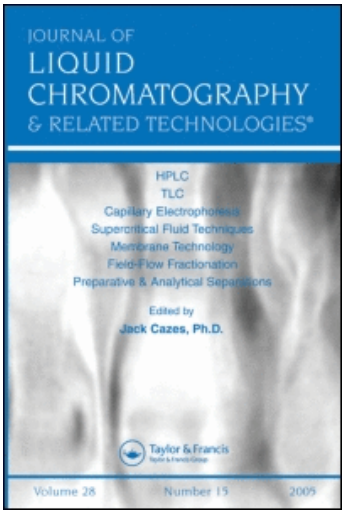

Journal of Liquid Chromatography & Related Technologies
Publication details, including instructions for authors and subscription information:
http://www.informaworld.com/smpp/title~content=t713597273

Non-Woven Electrostatic Media for Chromatographic Separation of Biological Particles

Fred Tepper[a]; Leonid Kaledin[a]; Tatiana Kaledin[a]
[a] Argonide Corporation, Sanford, Florida, USA

To cite this Article Tepper, Fred , Kaledin, Leonid and Kaledin, Tatiana(2009) 'Non-Woven Electrostatic Media for Chromatographic Separation of Biological Particles', Journal of Liquid Chromatography & Related Technologies, 32: 5, 607 — 627
To link to this Article: DOI: 10.1080/10826070802711006
URL: http://dx.doi.org/10.1080/10826070802711006

Journal of Liquid Chromatography & Related Technologies®, 32: 607–627, 2009

ISSN: 1082-6076 print/1520-572X online
DOI: 10.1080/10826070802711006

Non-Woven Electrostatic Media for Chromatographic Separation of Biological Particles

Fred Tepper, Leonid Kaledin, and Tatiana Kaledin

Argonide Corporation, Sanford, Florida, USA

Abstract: Nano alumina fibers, 2 nm in diameter and approximately 0.25 μm long are electroadhesively grafted to a microglass fiber. A non-woven media is formed by conventional wet-laid paper making technology. The media has a high affinity for virus, DNA/RNA, proteins, endotoxins, and antigens. A model was developed using data from adsorption of 30 nm latex spheres and was verified with MS2 coliphage.

The media is capable of separating equal size α3 and MS2 viruses. The process may be used for concentration and separation of biological particles, at high rates of flow and at pressures less than ~1 bar over ambient.

Keywords: DNA, Electrostatic adsorption, Filtration, Protein, RNA, Virus

INTRODUCTION

Non-woven media are often referred to as depth filters, because a particle has to traverse hundreds of pores before passing through the filter. They can be pictured as a series stack of filters, providing redundancy in depth. A defect at one level is compensated by layers beneath as compared to membranes, where a point defect can result in substantial increases in leakage.

Correspondence: Leonid Kaledin, Argonide Corporation, Nanomaterial Technologies, 291 Power Court, Sanford, Florida 32771, USA. E-mail: kaledin@argonide.com

Electroadhesive adsorption is a mechanism that is less dependent upon pore size than is the case with membranes or with typical depth filters. For decades, asbestos, an electropositive fiber, was used in non-woven filters until concerns about its carcinogenicity surfaced. Since then there have been many attempts to find a substitute electropositive filter. Membranes have been surface modified to provide some electropositive functionality, but because of their limited surface area, the benefits provided by such functionality are marginal. A non-woven filter format is best suited for separation via electroadhesion. The Cuno Corporation is the leader in such technology.

Electroadhesion utilizes the difference in charge that may exist between a membrane surface (or fiber) and a particle in an aqueous solution, where a charge is built up by the double layer effect. The zeta potential is a measure of the driving force between the particle and the fixed surface, acting to attract or repel the two. Most bacteria and most other particles are electronegative in water. The zeta potential tends to become more electronegative as the particle size decreases. The presence of salts and/or a moderate pH can adversely affect the electroadhesive function of commercially available electropositive media.

A novel water purification filter has been in development over the past eight years. The filter's active component is a nano alumina monohydrate fiber (AlOOH), only 2 nm in diameter. The isoelectric point of raw fibers is approximately 11.1.[1] Particles with an electronegative charge are attracted and retained by the nano alumina.

The nano alumina has been extensively used for decades as an adjuvant in vaccines[2] where the nano alumina serves as a carrier of antigens. Greater than 2 billion injections have been injected into human muscle tissue and countless more into domestic animals. The AlOOH (also known as Alhydrogel) is dissolved by citrate ion,[3] and is carried to the kidney where the aluminum is eliminated.

Figure 1 shows the TEM image of the nano alumina bonded to a microglass fiber. The nano alumina appears as a fuzzy layer on the microglass core. Polymeric fibers, primarily polyester plus cellulose, are added to the microglass/nano alumina composite for improved formability and pleatability. The nano alumina fiber content is optimized at 35 weight percent, so that the nano alumina fibers completely occupy the available surface of the 0.6 μm microglass fiber scaffolding, thus increasing the density of exposed electropositive charges that would collect electronegative particles. Early in the development of the media, the zeta potential for a 35 wt% sheet was in the range of +30 mV. As the manufacturing process became more refined, the zeta potential increased to about +50 mV.

The filter media is about 0.8 mm thick, resulting in approximately 400 pores that a particle must transit before exiting as filtrate. The combination of a dense attracting field and a tortuous path before exiting,

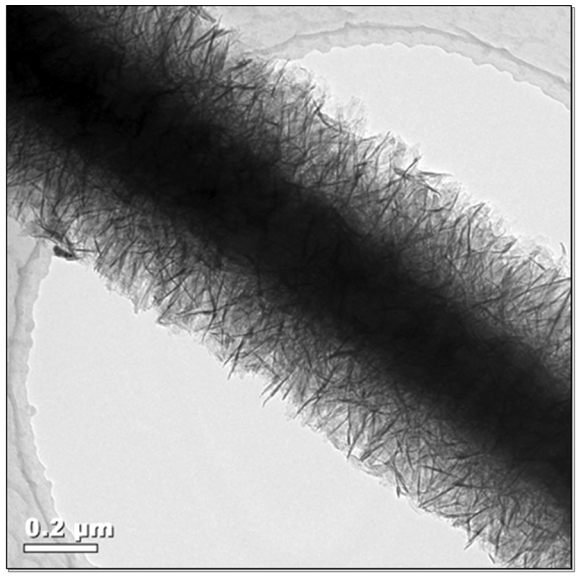

Photo courtesy of R. Ristau, IMS, Univ. of Conn.

Figure 1. TEM image of nanoalumina bonded to microglass fibers.

increases the retentivity of a particle so that it is equivalent or better than an ultraporous membrane, yet the flowrate is equivalent to a 2 μm depth filter; the large density of positive charges results in a high capacity for retaining sub-micron or nanosize particles.

Figure 2 shows a filter media that had been immersed in a concentrated solution of T4 phage for four hours and was washed with ethanol. This phage has an ovoid head approximately 60 nm across and 90 nm long.[4] A tail extends out about 200 nm. Note that the phage particles are crowded onto the media and appear to be tightly attached even after a 5 minute wash with ethanol. There is a growing consensus that coliphages can be used as indicator organisms for the presence of human pathogenic viruses,[5–9] much in the same way as coliforms are used to indicate the possible presence of bacterial pathogens.

This paper describes the development of an adsorption model. The fit of experimental virus adsorption data suggests a more extensive model that would describe both adsorption/desorption, aka, a mass transfer model that would be similar to those describing liquid chromatography. Data are provided where two nearly identically sized coliphages, α3 and MS2, are separated by displacement with a beef extract containing solution, or by elution with sodium carbonate. The data suggest that the media could be used for concentration and separation of biological

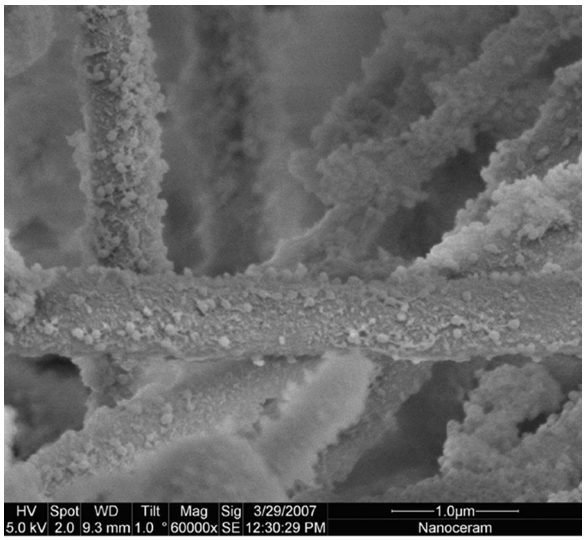

Courtesy E. Helmke, Alfred Wegener Institute, Germany

Figure 2. T4 phage attached to nano alumina/microglass fiber.

particles, at high rates of flow and at pressure drops less than ~1 bar over ambient. The resulting benefits would be substantial reduction in the cost and complexity in the downstream process liquid chromatographic separation of biological substances.

EXPERIMENTAL

Media Characteristics

X-ray diffraction patterns have identified the monohydrated nano alumina as predominantly pseudoboehmite (AlOOH). TEM's show the fibers to be 2 nm in diameter and approximately 0.25 μm long, that are electroadhesively grafted to a microglass fiber. The surface area, computed from the external surface of the 2 nm fiber, is about 600 m^2/g, and its BET surface area ranges between 200 and 550 m^2/g. This suggests that most of the surface area is external and accessible to particles and macromolecules, as compared to granular sorbents, where most of the surface area is within internal pores and unavailable to particles and large macromolecules. The pore size of the media (NanoCeram® or NC) can be varied from about 1 to 30 μm, although a 2–3 μm pore size was selected for purifying drinking water. The media has a rapid dynamic response for adsorbing bacteria, virus, and nucleic acids from biological

solutions. Typically, 5 LRV (logarithm reduction value) of bacteria and 4 LRV of viruses are retained by a pleated 0.8 mm thick layer at $25\,L/m^2/min$ at a ΔP of 0.4 bar. Most bacteria are large enough to be mechanically filtered, but smaller particles such as virus, protein, and nucleic acids are retained principally by electroadhesion.

The media can be modified by addition of ultra fine or nano size particles to the formulation. This innovation has resulted in a media containing powdered activated carbon (PAC, average particle size $\sim$8 microns). This PAC media has a high dynamic adsorption efficiency as compared to granular carbon media. It has been commercialized and has been certified under NSF/ASI Standard 53 as being safe for use in purifying drinking water.[10]

Media containing silica ($\sim$15 nm), nano titanium dioxide ($\sim$10 nm), and RNA have been integrated into the nano alumina media to produce other media with alternative adsorption properties.

Streaming and Zeta Potentials

Zeta potential (ζ) is an important and reliable indicator of the surface charge on the media and is a useful tool for the prediction of its adsorption efficiency for various particles. Zeta potential cannot be measured directly, but must be deduced from experimental data with the use of an appropriate model. The zeta potential can be determined by standard electrokinetic methods such as streaming potential.[11] Streaming potential is the electric potential that is developed when a liquid is forced through a network of pseudo capillaries within the matrix of the media. The fluid flow across the porous medium creates a potential that could be measured by using a pair of electrodes.

The streaming potential apparatus was similar to that described in Ref. [11]. The streaming potential was measured by means of a pair of Ag/AgCl electrodes located on both part of the filter at pH $\sim$7. The solution of a known conductivity as measured by Oakton ECTestr Pure (Fisher Scientific, resolution 0.1 $\mu S/cm$) is placed in a pressurized vessel and pressure is applied to the vessel and, therefore, to the filter. The streaming potential is found by applying at a given time an over pressure (ΔP, bar) to the vessel and measuring resulting potential difference ($\Delta\phi \equiv E_s$, V) on both sides of the filter disc. The E_s and ΔP values are measured at ± 1 mV and ± 0.03 bar, respectively, for virgin NC filters and filters loaded with fumed silica (Cab-O-Sil) and RNA as a function of pressure drop for water with conductivities of 1.3, 1.8, and 20.2 $\mu S/cm$.

It has been long recognized[12] that in the capillary flow situation the apparent zeta potential (ζ) is a function of bulk conductivity of filtered liquid (λ_b) while the true zeta potential (ζ_{true}) is a function of bulk

Table 1. Zeta potential and surface conductance of different NanoCeram media

Weight % NanoCeram on glass	Additive	Weight % of additive	Pore size, μm	True zeta potential, mV	Surface conductance λ_s, nS
40		0	2	29[a]±5	0.4±0.2
38		0	2	54[b]±6	1.3±0.7
26	PAC[c], APS[d] ~8 μm	32	3	47[b]±5	3.8±1.7
29	Fumed silica[e] APS[d] ~15 nm	28	2	56[a]±6	2.1±1.0
29	TiO_2 APS[d] ~5 nm	29	2	31[a]±4	3.8±1.7
30	TiO_2 APS[d] ~5 nm	20	2	35[a]±4	2.8±1.4
35	RNA from Torula yeast	5	2	−5.7[a]±4	0.04±0.04

[a]data for laboratory handsheet.
[b]data for manufactured material.
[c]powder activated carbon.
[d]average particle size.
[e]Cab-O-Sil.

conductivity of filtered liquid (λ_b) as well as surface conductance effect due to the capillary tube material (λ_s).

The manufactured NC media has a zeta potential typically in the range of +50 mV at pH 7 (see Table 1). Approximately 5% RNA (torula yeast, Sigma-Aldrich) was added to the slurry in forming hand sheets prepared using a method similar to that described in the standard TAPPI method.[13] Streaming potential measurements showed that the hand sheet had become electronegative ($\zeta = -5.7$ mV).

Zeta Potential and Virus Retention

Table 2 shows the affect of increasing the ratio of nano alumina to microglass on the zeta potential as well as on the retention of MS2 (icosahedral virus with diameter 27.5 nm,[14] (ATCC® 15597-B1™) and PRD-1 (the smallest dimension is 66 nm between opposing faces and the largest is 74 nm between opposing vertices,[15] ATCC 824) coliphages. The filters in these experiments were ~1.6 mm thick and the flow rate was 10 mL/cm^2/min. Note that pure microglass fiber, which is electronegative, is very ineffective for filtering MS2 virus. As the ratio of nano alumina increases, the charge becomes positive. At about 15 weight percent (wt%) alumina, virus retention becomes very high. At about 50 wt% nano alumina, the surface of a 0.6 μm glass fiber is saturated with nano alumina fibers.

Table 2. Zeta potential and virus removal

Weight % NanoCeram on glass	True zeta potential (mV)	MS-2 % removal	PRD-1 % removal
0	−35	8	Not done
5	−10	29	Not done
10	7	94	Not done
15	15	>99.9999	>99.99999
25	35	>99.9999	>99.99999
40	29	>99.9999	99.99991
50	23	>99.9999	>99.99999

Table 3 shows the retention of the filter media for MS2 phage as compared to a competitors electropositive media, which has been used for virus filtration applications for several years. A filter disc of the NC media was compared to a double layer of the competitor's media, so as to have a similar basis weight. Each filter was continuously challenged with MS2 solution. Ten milliliter aliquots were collected from solutions passed through 25 mm discs at a rate of 160 $L/m^2/min$ and were assayed for phage by a conventional soft agar overlay method.[16] Note that the NC media maintained a high level of phage retention at pH 9.2 and also in the presence of 30 g/L of dissolved salt, while the competitive media was almost transparent to the phage under these conditions.

Table 3. MS2 removal by electropositive media

			Challenge water			MS2 removal,%		
Media	Thickness (Mm)	Basic weight (g/m^2)	pH	TDS[a] (g/L)	MS2[b] (PFU/mL)	0–10 (mL)	60–70 (mL)	130–140 (mL)
NC Filter	0.8	220	7.2±0.1	0	$6 \cdot 10^5$	99.5	99.5	99.8
			9.2±0.1	0	$5 \cdot 10^5$	99.0	96.2	
			7.2±0.1	30	$5 \cdot 10^5$	99.4	98.6	
			9.2±0.1	30	$4 \cdot 10^5$	97	90	
Other electro-positive filter	0.8[c]	210[c]	7.2±0.1	0	$6 \cdot 10^5$	99.3	92	62
			9.2±0.1	0	$3 \cdot 10^5$	60	13	
			7.2±0.1	30	$5 \cdot 10^5$	4	6	
			9.2±0.1	30	$4 \cdot 10^5$	0	0	

[a]Total Dissolve Solids (TDS) – sea salts.
[b]MS2 input concentration; Plaque Forming Units (PFU).
[c]for double layer.

Adsorption of Nucleic Acids

Three different DNA solutions (500 μg/mL in 50 mL) were prepared using nuclease free water. The DNA used were: calf thymus (M. W. 6,000,000 ICN Biomedicals Inc., Ohio), E. coli (isolated by procedure of marmur, ICN Biomedicals Inc., Ohio), and salmon sperm (Fisher Bioreagents, Fair Lawn, NJ). NC filters discs (25 mm diameter, 1.2 mm thick) were mounted in filter holders. Water (100 mL) was passed through each of nine filters. Fifteen milliliters of the DNA solution was then passed through each filter at a flow rate of 15 mL/cm^2/min. The effluent was collected in nuclease free tubes. The DNA concentrations in filter effluents were measured using a Hoefer TKO 100 mini fluorometer (Hoefer Scientific Instruments, San Francisco). In every case the effluent had < 10 μg/mL of DNA with an average of 4.1 μg/mL, demonstrating a retention greater than 99% in all cases.

The filter's capacity was determined for calf thymus, *E. coli*, and salmon sperm DNA to be greater than 88 mg/g, 100 mg/g, and 88 mg/g, g, respectively, at greater than 99% recovery level and at input concentration of ~500 μg/mL (see Table 4). When BSA (bovine serum albumin) was passed through the filter prior to the test, DNA capacity was reduced by a factor of ~10. Presumably, the BSA competes for the same sites.

Breakthrough curves were developed for adsorption of RNA derived from torula yeast (Sigma-Aldrich) in a buffered Tris-EDTA solution

Table 4. Sorption capacity of NanoCeram® filter media

Adsorbate	Source	Influent concentration (mg/mL)	Sorption capacity to 99% of retention limit (mg/g)	Sorption capacity to 50% of retention limit (mg/g)
DNA	Calf Thymus	523	250[a] 88[b]	
	E. coli	610	290[a] 100[b]	
	Salmon sperm	541	250[a] 88[b]	
RNA	Torulla yeast	100	85[a] 30[b]	185[a] 65[b]
Protein	BSA[c]		85[a] 30[b]	1600–3100[a,d]
Endotoxins	*E. coli* endotoxin 055:B5	48[e]	3400[a] 1200[b]	

[a]with respect to weight of nanofibers.
[b]with respect to NanoCeram media.
[c]bovine serum albumin.
[d]Ref. (1).
[e]Reference Standard Endotoxin/Control Standard Endotoxin (RSE/CSE) ratio is 10 EU/ng.

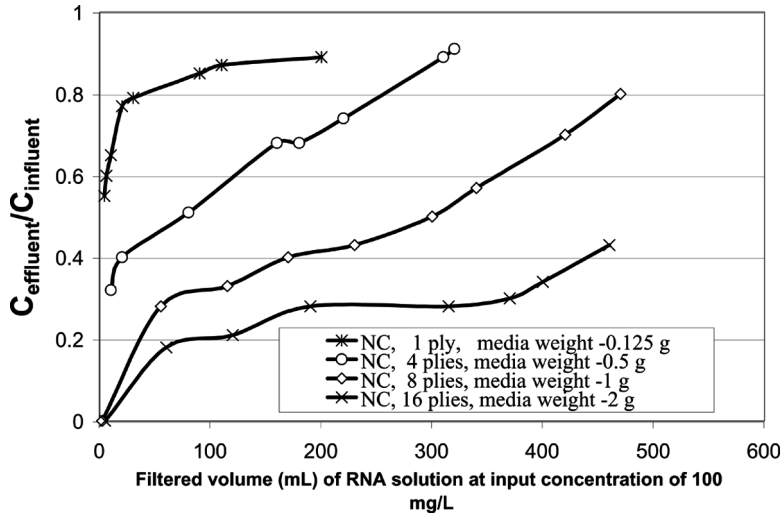

Figure 3. RNA (torula yeast) breakthrough curves.

(100 μg/mL at pH 8.0 ± 0.1). The blue fluorescent DAPI nucleic acid stain (Molecular Probes, fluoropure grade) was added to RNA solution. The excitation maximum for DAPI bound to RNA is 358 nm and the emission maximum is 500 nm. NC filters (25 mm diameter, 1-, 2-, and 4-plies) were challenged by aliquots of 0.3 mL to 15 mL of RNA/DAPI solution at a flow rate of 20 mL/min. The fluorescent signal was measured with the use of a Hoefer TKO-100 mini fluorometer. Figure 3 shows that the dynamic capacity is proportional to bed depth. The capacity for torula yeast RNA was measured as 30 mg/g at an input concentration of 100 μg/mL.

RESULTS AND DISCUSSION

Sorption Model

From the prospective of the design engineer, prediction of the breakthrough curve for a given filter, using only basic kinetic and equilibrium data is desirable. To extract dynamic information, the experimental adsorption isotherm(s) must be fitted to the theoretical response curve(s), calculated with a suitable dynamic model for the system. While the mechanism of adsorbing these relatively large macroscopic particles is understood in qualitative terms, we could find no quantitative descriptions of similar processes in the literature for the case where most of the surface area is external and accessible to particles and macromolecules,

as compared to granular sorbents, where most of the surface area is within internal pores and unavailable to particles and large macromolecules.

A model was developed that describes the adsorption of virus and other particulates by the electropositively or electronegatively charged depth filter media and applied to the case of the new filter media. The surface area derived via BET adsorption for the nano alumina closely matched the calculated surface area assuming a 2 nm diameter. Helium adsorption showed less than 10% porosity. This indicates that the large surface area of the nano alumina fibers (up to $\sim 500\,m^2/g$) is on the surface and available for adsorption, like flagella, as seen in Figure 1. This permitted us to reduce the complexity of the diffusion solutions as compared to one for a porous solid, where there is complexity owing to particle migration below the surface, through micro- and macropores. Although the expressions for the breakthrough curves derived from different models are algebraically different, the numerical difference is quite small and it became a common practice to use the simpler linear driving force models to further simplify the algebraic solutions.[17]

We chose a general analytical solution (see Refs. [17–19]) by assuming that: (i) the nature of equilibrium relationship is linear; (ii) the nature of equilibrium is isothermal, i.e., heat transfer resistance can be neglected; (iii) the concentration level of the adsorbable component is relatively low such that it does not influence basic properties of the carrier liquid, e.g., viscosity, conductivity, etc.; (iv) the flow model is an ideal plug flow system when the axial dispersion term $-D_L\partial^2 c/\partial z^2$ can be neglected, thereby, reducing the mass balance equation to a first order hyperbolic equation;[17] (v) the kinetic model assumes negligible mass transfer resistance due to the fact that instantaneous equilibrium can be assumed at all points because of the open character of the filter media. Under these assumptions, the analytical solution for a breakthrough curve is given by the following asymptotic equation (see e.g. Ref. [17]):

$$c_b^+ = \frac{1}{2}\left(1 - erf\left(\sqrt{z^+} - \sqrt{\theta^+}\right)\right) \quad \text{for } z^+ \geq \theta^+ \quad \text{for} \quad z^+ >> 1 \qquad (1)$$

where $c_b{}^+ = c_b/c_0$ is dimensionless concentration
c_0 is challenge concentrationc_b is bulk concentration
θ^+ is a dimensionless value of corrected time θ defined as $t\text{-}z \cdot \varepsilon/v$
z^+ is a dimensionless value of z
z is depth of the media
ε is porosity of the media
v is flow velocity
erf is the error function

Equation (1), therefore, allows prediction of a breakthrough curve for large values of z^+ from constants derived from experimental measurements of the dynamic adsorption isotherms. To characterize

the adsorption process of small particles by a given depth filter media, a specific model can be constructed in the following way: (i) measure dynamic adsorption isotherms for a given thickness of media for at least three input particle concentrations at the same flow rate, pH, amount of total dissolved solids (TDS), etc.; (ii) fit dynamic adsorption isotherm to Eq. (1), which allows determination of the value of z^+ and filter capacity; (iii) fit the capacity values to the Freundlich and/or Langmuir isotherm.

Adsorption of Monodisperse Latex Beads

First we tested the above model using adsorption data of 30 nm monodisperse polystyrene latex beads at challenge concentrations between 10^{12} to 10^{13} particles/mL, over a pH range of 5–10 and at one specific flux of 1.6 mL/cm^2/min through a 3.7 cm^2, 1.6 mm thick NC disc. The particle removal efficiency of the media sample can be calculated directly from the inlet and effluent turbidity values. These tests use relatively high contaminant challenge levels to reduce the time to breakthrough. We found that in the case of 30 nm latex beads, Equation (1) accurately describes breakthrough curves at a residence time greater than about 0.1 second through the filter. Table 5 presents values of z^+ and filter capacity for 30 nm latex beads obtained from the fits of the breakthrough curves.

Table 5. Values derived from latex bead breakthrough curves

Input concentration, beads/mL	pH	Filter capacity, 10^{14} beads	z^+
$1 \cdot 10^{12}$	5	0.83	27
	7	0.96	26
	9	1.17	49
	9.5	0.55	36
	10	0.31	26
$4 \cdot 10^{12}$	5	1.24	30
	7	1.44	30
	9	1.32	33
	9.5	0.76	16
$3 \cdot 10^{12}$	10	0.81	16
$1 \cdot 10^{13}$	5	1.45	10
	7	1.45	20
	9	2.25	16
	9.5	1.4	15
	10	1.5	23

Table 6. Langmuir isotherm parameters

pH	$q_m/10^{14}$, beads[a]	$b \cdot 10^{12}$, mL/beads[a]
5±0.1	1.59±0.04[b]	1.0±0.2
7±0.1	1.52±0.06	2.3±1.2
9±0.1	2.66±0.88	0.42±0.39
9.5±0.1	1.81±0.68	0.28±0.18
10±0.1	2.54±0.22	0.15±0.01
Average value[c]	1.59±0.08	0.91±0.15

[a]parameter values were obtained by fitting the experimental data to Langmuir equation (2).
[b]standard deviation (1σ).
[c]average value calculated from the first three entries (neglecting pH 9.5 and 10).

Filter capacity values of Table 5 were then compared to the Langmuir expression:[20]

$$c/q = 1/(b \cdot q_m) + 1/q_m \cdot c \quad (2)$$

where q_m is the maximum adsorbed phase concentration when all the adsorption sites are occupied and $b = k_a/k_d$ where k_a and k_d are the adsorption and desorption coefficients. The fit of experimental data to the Langmuir isotherm for pH's between 5 and 9 was found to be within 1 s of the average, while the q_m for pH 10 was $> 3\sigma$ from the average (see Table 6).

The fit of experimental data of Table 5 to the Freundlich empirical isotherm (see Equation (3)) for pH's between 5 and 9 was found to be within $1\,\sigma$ of the average (compare values of log K and 1/n for different pH's), while the values of log K and 1/n for pH 9.5 and 10 was $> 3\,\sigma$ outside from their average values (neglecting data for pH 9.5 and 10, see Table 7):

$$q = K \cdot c^{1/n} \quad (3)$$

where K and n – are constants.

The Freundlich relationship is useful in that it develops a parameter K (Equation (3)) that is a measure of sorption capacity and a parameter (1/n) that is a measure of adsorption strength.[20] Within the accuracy of the experiment, the highest capacity and strongest bond for latex beads was obtained at pH from 5 to 9, with considerable divergence from average values for a pH of 9.5 and higher (see Table 7). These conclusions are similar to those derived from the Langmuir isotherm analysis (see Table 6).

Table 7. Freundlich isotherm parameters

pH	log K[a]	K	1/n
5.0±0.1	10.98±0.41[b]	$9.5 \cdot 10^{10}$	0.25±0.03[b]
7.0±0.1	11.74±0.98	$5.5 \cdot 10^{11}$	0.19±0.08
9.0±0.1	10.81±1.7	$6.5 \cdot 10^{10}$	0.27±0.13
9.5±0.1	9.00±1.5	$1.0 \cdot 10^{9}$	0.39±0.12
10.0±0.1	5.3±1.1	$2.0 \cdot 10^{5}$	0.69±0.09
Average value[c]	11.08±0.14	$12 \cdot 10^{10}$	0.244±0.010

[a]parameter values were obtained by fitting the experimental data to Freundlich equation (3).
[b]standard deviation (1σ).
[c]average value calculated from the first three entries (neglecting data for pH 9.5 and 10).

Adsorption of MS2 Viruses

The model was also tested via Equation (1) with MS-2 virus at different flow rates and different virus input concentrations at neutral pH 7. Model parameters q and z^+ were determined by fitting procedure for each individual breakthrough curve and then those parameters were correlated to the following equations assuming Freundlich empirical isotherm (see Equation (3)) and neutral pH 7.

$$q = 5.9 \cdot 10^7 (\text{PFU}) \cdot (z_m(\text{mm})/z_0) \cdot C^{0.323} \quad (4)$$

$$z^+ = 88(\text{mm}^{-1} \cdot \text{min}^{-0.5}) \cdot z_m(\text{mm}) \cdot (v(\text{mm/min}))^{-0.5} \quad (5)$$

where z_m is thickness of the media

C is MS2 concentration (PFU/mL)

$z_0 = 1.6\,\text{mm}$

Equations 1, 4, and 5 permit calculation of breakthrough curves at pH 7 for MS2 input concentrations in the range from 10^3 PFU/mL to 10^{10} PFU/mL and at residence times ($= z_m/v$) greater than about 0.1 sec.

The model was also tested via Equations (1, 4, 5) with MS2 virus at two different flow rates. In the first series the challenge solution consisted of 40 mL of $\sim 1.9 \cdot 10^7$ MS2/mL, flowing at a constant flow velocity of $\sim$10 cm/min, through a 25 mm diameter filter disc. The thickness' tested were 0.4 mm (one ply), 0.8 mm (two plies), 1.2 mm (three plies), or 1.6 mm (four plies) filters. In the second series, the challenge solution was 40 mL of $\sim 1 \cdot 10^6$ PFU/mL MS2 virus, flowing at a constant flow velocity of 40 cm/min. Figure 4 compares experimentally derived LRV with projected performance from the model, as a function of

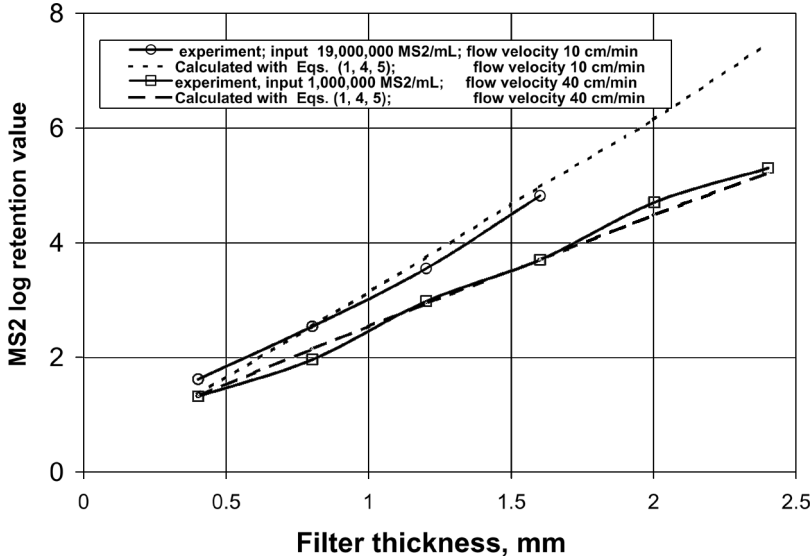

Figure 4. Experimental LRV compared to projected performance from the model.

bed thickness, for the two different flow rates of 10 & 40 mL/cm^2/min. The close agreement suggests that the model can be used with different solutes. One we tested was RNA, where we also found good conformance.

The fit of experimental data with the model suggests that adsorption has near ideal conformance with mass transfer equations at residence times through the filter greater than 0.1 second. This suggests that a mass transfer equation could be developed that describes the chromatographic process, and that such a model would be applicable to particles other than virus.

Separation of Viruses

We elected to demonstrate feasibility of chromatographic use by separating two small coliphage viruses MS2 and a3 (ATCC® 13706-B2) that have nearly identical particle size of, respectively, ~27 nm[12] and ~25 nm.[21] Both viruses are uncapsided. We also chose to use conventional culture to assay the viruses in eluted fractions. With live viruses, we would be assured that the particle was not affected in transit through the separation process.

We tried two types of eluents. The first was a solution of 3% beef extract, 0.25% glycine, and at a pH of 9.3. This solution had been developed earlier for extracting virus from electropositive media. Protocols are being developed by EPA[22] and others for assay of norovirus, adenovirus, polio, and bird flu using this or similar eluents. The second eluent was a 0.025 *M* sodium carbonate solution (pH ~10).

NC discs, 25 mm in diameter, were loaded with a mixture of approximately equal quantities of MS2 and α3 viruses at input concentrations from 100 to1000 phage particles/mL at a flow rate of 10 mL/min. Elutions were performed by passing 0.25–2.5 mL aliquots of beef extract solution through a stack of 1, 6, and 12 layers of the same filter media at a flow velocity of 1 cm/min in the same flow direction as the adsorption step. Results are shown in Figures 5–7.

Figures 5–7 show that the separation of the two viruses improves with increasing thickness of the media. Separation is effected at flow velocities of 1 cm/min and at less than 1 bar that are small fractions of that in HPLC separation. Further separation of virus would occur if more than 12 layers were used.

A solution of 0.025 *M* Na_2CO_3 was prepared by dissolving sodium carbonate in reverse osmosis purified water and then filtering the solution through a 0.45 mm membrane. As with beef extract elution experiments, a single disc and stacks of 3 and 6- layers discs (25 mm in diameter) were

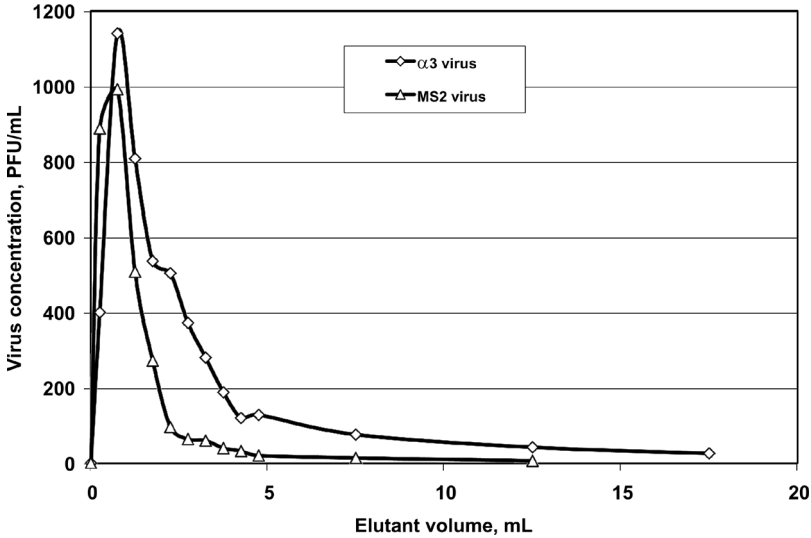

Figure 5. α3 and MS2 viruses eluted through 1 layer of NC disc at flow velocity 1 cm/min.

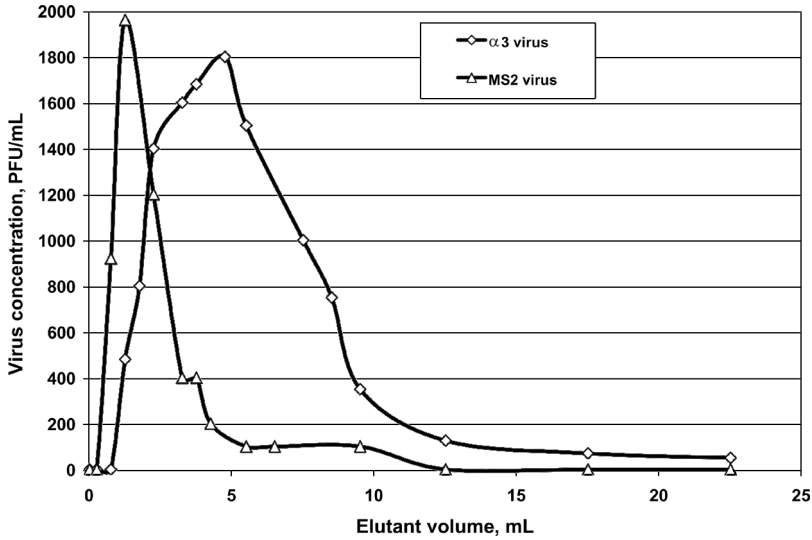

Figure 6. α3 and MS2 viruses eluted through 6 layers of NC discs at flow velocity 1 cm/min.

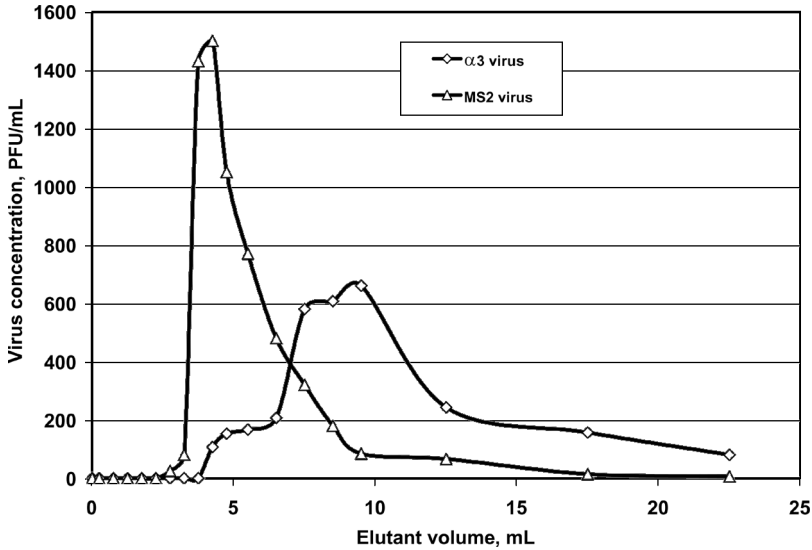

Figure 7. α3 and MS2 viruses eluted through 12 layers of NC discs at flow velocity 1 cm/min.

loaded with mixtures of MS2 and α3 viruses at input concentrations in the range of 100 to 500 agent particles/mL, and at a flow rate of 10 mL/min. Elutions were performed by passing 0.5 mL aliquots of eluent at a flow rate of 5 mL/min in the same flow direction as the adsorption step. The data (not shown) indicate that the degree of separation of two viruses improves with increasing thickness of the media, similar to that eluted with beef extract/glycine. However, pressure drop during the elution step with sodium carbonate was consistently higher than in the case of beef extract/glycine eluent. It is likely that at high pH ~10 some portion of the NC fibers was lifted from the microglass and the NC fibers were traveling downstream of the media resulting in its partial clogging.

Elution of RNA With Na_2CO_3

NC discs (25 mm diameter, 0.8 mm thick) were loaded with 5 mL of RNA (torula yeast, Sigma, Catalog # R6625) solution at input concentrations of 500 μg/mL and at a flow rate of 10 mL/min. Elutions were performed by passing 2 mL aliquots of 0.01 *M*, 0.025 *M*, and 0.5 *M* solutions of Na_2CO_3 at a flow rate of 5 mL/min and at a pressure drop of approximately ~4 psi. The flow direction was opposite to that of the adsorption experiments. The blue fluorescent DAPI nucleic acid stain (Molecular Probes, fluoropure grade) was added to the RNA in the effluent. The excitation maximum for DAPI bound to RNA is 358 nm and the emission maximum is 500 nm. It is known, that the DAPI stain while

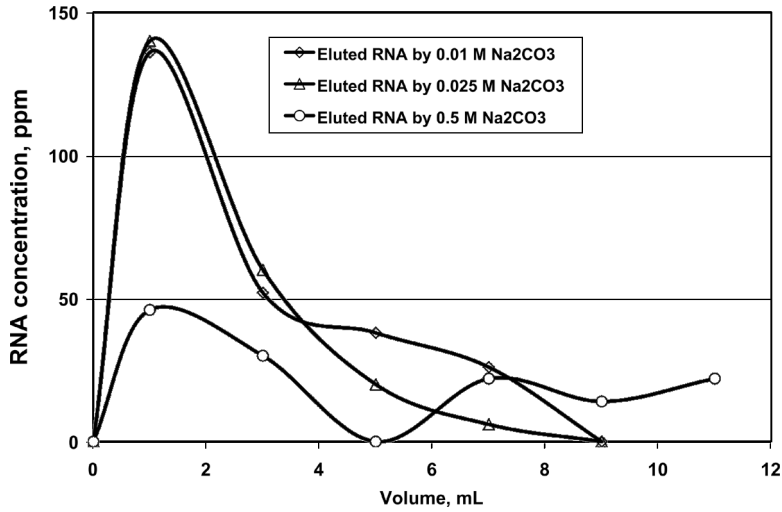

Figure 8. RNA (torula yeast) eluted with reverse flow by Na_2CO_3 from one disc.

bound to dsDNA increases the resulting fluorescence signal by a factor of 20. Similar behavior is noted when the DAPI stain is bound to the RNA molecules. The fluorescent signal was measured with the use of a Hoefer TKO-100 fluorometer. Results are reported in Figure 8 at a resolution of 2 mL.

The data show that there is a sharp peak at about 1 mL, during the elution of RNA from NanoCeram media that does not depend on the concentration of Na_2CO_3 with a maximum at 1 mL per 3.7 cm^2 of filtration surface area.

CONCLUSIONS

This paper demonstrates how the strong inherent electropositive charge properties of nano alumina fiber media can be used in separation of viruses and other suspended particulates. The media adsorbs submicron particles predominately on the basis of their charge, rather than by physical entrapment based on particle size. The media has a high dynamic response for adsorption, allowing purification within a very shallow bed, and doing so at a pressure below 1 bar over ambient and at flow rates an order of magnitude or greater than can be achieved with an ultraporous membrane.

The adsorption step is repeatable. This facilitated the development of a model that describes the adsorption process as a function of particle concentration, bed thickness, and flow velocity. The model has proven useful in developing dynamic adsorption data for a new particle, by obtaining its isotherm for a given matrix.

A given particle can be eluted by replacement with one that is more adherent. For instance, viruses can be lifted off the media by replacement with beef extract. Alternatively, sodium carbonate solution has also been effective as an eluent, although it is suspected that the nano alumina structure is adversely affected.

The media can also be modified by adding functionality or grafting various nanoparticles to it. Callender et al.[23] describes the attachment of ligands to boehmite (AlOOH) fibers using the carboxy group. He synthesized "water soluble" carboxylate-alumoxane precursors from inexpensive boehmite feed stock. Carboxylate-alumoxanes, $[Al(O)_x(OH)_y(O_2CR)_z]_n$, were synthesized by the reaction of boehmite, $[Al(O)(OH)]_n$, with acetic acid (CH_3CO_2H), methoxyacetic acid ($HO_2CCH_2OCH_3$), or (methoxyethoxy)acetic acid ($HO_2CCH_2OCH_2CH_2OCH_3$). We have treated the nano alumina (boehmite) with glacial acetic acid to produce a surface that exhibited hydrophobic properties.

Another alternative is the grafting of a biological particle onto the sheet during its formation, as is described above for RNA. Such particles

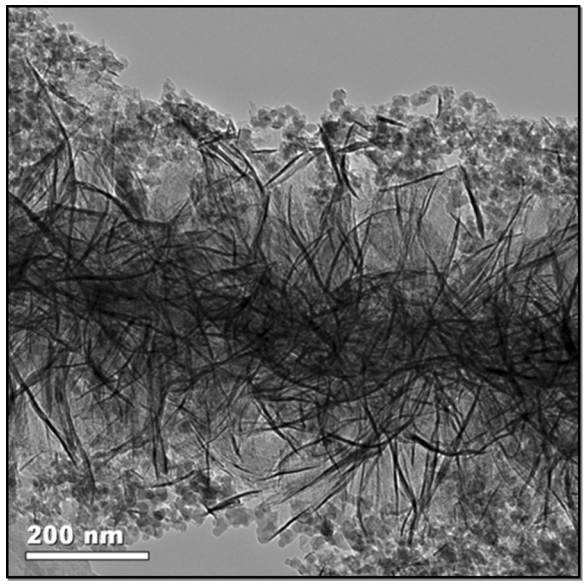

Figure 9. Nanosilica deposited on nano alumina/microglass fiber.

might be an antibody or an aptamer that could target various small molecules, proteins, nucleic acids, or virus.

Nanosize inorganic oxides can be added to the sheet to alter its sorption characteristics. Figure 9 shows silica particles approximately 10 nm that cover the nano alumina. The loading of the silica in the micrograph was 28 wt%. The silica is electronegative at $pH > 2$ and it had been anticipated that when added to the nano alumina, its zeta potential would tend to be more negative. On the contrary, the zeta potential (see Table 1) was found to become more electropositive (+56 mV). Such a media would have far more surface area than silica beads used in HPLC. Moreover, the diffusion effects within such a structure would be significantly limited because the electrostatic fields project out into the pore space by about as much as 0.3–0.5 microns as predicted by Equation (6) (see Ref. [12]) at low ionic strengths of aqueous solutions.

$$\delta = 0.303\text{nm}/(\text{ionic strength})^{1/2} \tag{6}$$

The experimental results also suggest that the nano alumina media can be used for clarification of solutions from cell debris, nucleic acids, and for sterilization. The data also suggest that the media should effectively remove viruses from blood plasma proteins, recombinant proteins

from cell culture media, and monoclonal antibodies. Such separations can occur in ionic solutions. The media is suggested for purification of virus and proteins, where a high dynamic binding capacity is combined with flow velocities an order or two greater than is achievable with membrane separation, and at low back pressure. Chromatographic separations at pressure drops less than ~1 bar over ambient, in thin beds and with high flow rates, appear feasible.

REFERENCES

1. Al-Shakhshir, R.; Regnier, F.; White, J.L.; Hem, S.L. Effect of protein adsorption on the surface charge characteristics of aluminium containing adjuvants. Vaccine. **1994**, *12* (5), 472–474.
2. Glenny, A.T.; Pope, C.G.; Waddington, H.; Wallace, U. The antigenic value of the toxoid precipitated by potassium alum. J. Pathol. Bacteriol. **1926**, *29*, 31–40.
3. Petrovsky, N.; Aguilar, J.C. Vaccine adjuvants: current state and future trends. Immunol. Cell Biol. **2004**, *82* (5), 488–96.
4. Fokine, A.; Chipman, P.R.; Leiman, P.G.; Mesyanzhinov, V.V.; Rao, V.B; Rossmann, M.G. Molecular architecture of the prolate head of bacteriophage T4. Proc. Natl. Acad. Sci. USA. **2004**, *101* (16), 6003–6008.
5. Stetler, R.E. Coliphages as indicators of enteroviruses. Appl. Environ. Microbiol. **1984**, *48* (3), 668–670.
6. Gerba, C.P. Phage as indicators of fecal pollution, in *Phage Ecology*; Goyal, S.M., Gerba, C.P., Bitton, G., Eds.; Wiley-Interscience: New York, 1987; 197–209, 321.
7. Palmateer, G.A.; Dutka, B.J.; Janzen, E.M.; Meissner, S.M.; Sakellaris, M.G. Coliphage and bacteriophage as indicators of recreational water quality. Water Res. **1991**, *25*, 355–357.
8. Havelaar, A.H. Bacteriophages as models of human enteric viruses in the environment: although imperfect, phages can act as sentinels for a safer water supply. Am. Soc. Microbiol. News. **1994**, *12*, 614–619.
9. Havelaar, A.H.; van Olphen, M.; Drost, Y.C. F-specific RNA bacteriophages are adequate model organisms for enteric viruses in fresh water. Appl. Environ. Microbiol. **1993**, *59* (9), 2956–2962.
10. Frank, H. Another twist in filtration for high-purity and other systems. A filter media combines nano-alumina and powdered activated carbon. Water Technol. **2008**, *31* (9), 32–36.
11. Oulman, C.S.; Baumann, E.R. Streaming potentials in diatomite filtration of water. J. AWWA **1964**, (July) 915–930.
12. Mossman, C.E.; Mason, S.G. Surface electrical conductance and electrokinetic potentials in networks of fibrous materials. Can. J. Chem. **1959**, *37*, 1153–1164.
13. *TAPPI Test Methods 2000–2001*, Method T-205. Forming handsheets for physical tests of pulp, TAPPI press: Atlanta, USA, 2000.

14. Golmohammadi, R.; Valegård, K.; Fridborg, K.; Liljas, L. The refined structure of bacteriophage MS2 at 2.8A resolution. J. Mol. Bio. **1993**, *234*, 620–639.
15. Butcher, S.J.; Bamford, D.H.; Fuller, S.D. DNA packaging orders the membrane of bacteriophage PRD1. The EMBO J. **1995**, *14* (24), 6078–6086.
16. Pepper, I.L.; Gerba, Ch.P.; Brendecke, J.W. *Environmental Microbiology. A Laboratory Manual*; AP: San Diego, 1995; 175.
17. Ruthven, D.M. *Principles of Adsorption and Adsorption Processes*; Wiley-Interscience: New York, 1987; 464.
18. Walter, J.E. Rate-dependent chromatographic adsorption. J. Chem Phys. **1945**, *13*, 332–336.
19. Thomas, H.C. Heterogeneous ion exchange in a flowing system. J. Am. Chem. Soc. **1944**, *66*, 1664–1666.
20. Atkins, P.W. *Physical Chemistry*; W. H. Freeman and Co.: San Francisco, 1978; 1022.
21. Bernal, R.A.; Hafenstein, S.; Olson, N.H.; Bowman, V.D.; Chipman, P.R.; Baker, T.S.; Fane, B.A.; Rossmann, M.G. Structural studies of bacteriophage alpha-3 Assembly. J. Mol. Biol. **2003**, *325*, 11–24.
22. *USEPA Manual of Methods for Virology*, Chapter 14; April 2001.
23. Callender, R.L.; Harlan, C.J.; Shapiro, N.M.; Jones, Ch.D.; Callahan, D.L.; Wiesner, M.R.; MacQueen, D.B.; Cook, R.; Barron, A.R. Aquesous synthesis of water-soluble alumoxanes: environmentally benign precursors to alumina and aluminum-based ceramics. Chem. Mater. **1997**, *9* (11), 2418–2433.

Received September 30, 2008
Accepted October 21, 2008
Manuscript 6406